BIOCHEMISTRY
including biophysical chemistry & molecular biology

Article

pubs.acs.org/biochemistry

Structure of Mediator of RhoA-Dependent Invasion (MRDI) Explains Its Dual Function as a Metabolic Enzyme and a Mediator of Cell Invasion

Paul D. Templeton,[§] Elizabeth S. Litman,[#] Sandra I. Metzner,[§] Natalie G. Ahn,*[,§,#,⊥] and Marcelo C. Sousa*[,§]

[§]Department of Chemistry and Biochemistry, [#]HHMI, [⊥]BioFrontiers Institute, University of Colorado at Boulder, Boulder, Colorado 80309-0596, United States

Supporting Information

ABSTRACT: Metastatic melanoma is among the most intractable cancers to treat; patients show resistance to therapy and limited survival time. A critical step in the development of metastatic melanoma is the acquisition of invasion and transition from thin to thick tumors on the skin, followed by invasion to lymph nodes. Prior studies have shown that metastatic melanoma is associated with dysregulation of RhoA and enhanced expression of a protein named "mediator of RhoA-dependent invasion (MRDI)". Importantly, MRDI is a "moonlighting" enzyme, with two distinct functions in melanoma cells. First, MRDI acts as a methylthioribose-1-phosphate (MTR-1-P) isomerase, catalyzing a critical step in methionine salvage. Second, MRDI promotes and is necessary for melanoma cell invasion, independent of its catalytic activity. This paper demonstrates that MtnA, a bacterial MTR-1-P isomerase, rescues the methionine salvage function of MRDI, but is unable to rescue its role in invasion. The crystal structure of MRDI was solved to a resolution of 2.5 Å to identify structural elements important for its invasion activity. This structure and its comparison with other MTR-1-P isomerases are presented, and mutations within a region separate from the MTR-1-P binding site, which interfere with invasion, are identified. Thus, structural elements in MRDI distal from the MTR-1-P catalytic site are responsible for the invasion phenotype.

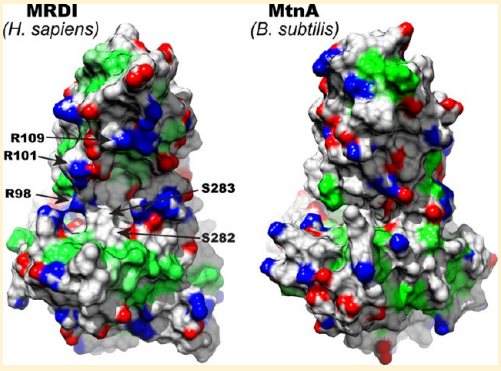

One of the most interesting outcomes emerging from the study of cellular proteomes is the identification of "moonlighting" proteins, which are proteins known to perform more than one function. Many examples involve metabolic enzymes, which show separate roles in diverse processes, including gene expression, signal transduction, and chaperone function.[1,2] Aconitase is a classic example, in which this TCA cycle enzyme also functions as an iron-responsive binding protein (IREBP), repressing translation of transferrin and other iron feedback inhibited proteins by binding the 5′-untranslated region of their mRNAs.[3] Initially, the number of moonlighting proteins was few and anecdotal, but with the increased numbers of functional annotations for proteins, in part due to large-scale screening results, the discovery rate for proteins associated with unexpected processes is increasing.[1] Therefore, the one protein−one function assumption is rapidly changing, and perhaps with new databases and data-mining studies, the existence of moonlighting proteins may be the rule, rather than the exception. However, in most cases, the mechanisms underlying moonlighting behavior remain unknown, lacking structural analyses that explain the molecular basis of how one protein can mediate vastly distinct cellular functions.

In studies of metastatic melanoma cells, functional proteomics was used to screen for proteins that responded to constitutive activation of the GTPase RhoA. A previously uncharacterized gene, named "mediator of RhoA-dependent invasion" (MRDI), was identified on the basis of its induction in response to RhoA and its ability to promote RhoA-dependent cell invasion in three-dimensional collagen matrices.[4] RNA interference showed that the expression of MRDI was necessary to allow tyrosine phosphorylation of focal adhesion kinase (FAK), an event that promotes kinase activation and cell motility.

Sequence alignments revealed a similarity between human MRDI and bacterial methylthioribose-1-phosphate isomerases. These enzymes function in methionine salvage by converting the *S*-adenosylmethionine metabolite, methylthioribose-1-phosphate (MTR-1-P), into methylthioribulose-1-phosphate (MTRu-1-P), which is ultimately converted to methionine in the salvage pathway.[4−6] The catalytic activity of MRDI as a MTR-1-P isomerase was demonstrated in vitro using NMR to identify the product. Furthermore, catalytic activity was abolished by mutations of residues Cys168 and Asp248, strictly conserved in MTR-1-P isomerases. In human cells, siRNA

Received: May 2, 2013
Revised: July 12, 2013
Published: July 16, 2013

   dx.doi.org/10.1021/bi400556e | *Biochemistry* 2013, 52, 5675−5684

depletion of MRDI, or mutation of its conserved Cys168 or Asp248 residues, abolished the ability of cells to grow in methionine-free media supplemented with methylthioadenosine (MTA), the metabolic precursor to MTR-1-P. This confirmed the primary role of MRDI in human cells as an MTR-1-P isomerase that mediates the methionine salvage pathway.

Although mutations at the Cys and Asp residues implicated in catalysis ablated MTR-1-P isomerase activity, neither affected invasion of cells within 3D spheroids encapsulated in collagen.[4] This revealed that MRDI has separate mechanisms for its metabolic and invasive functions and can thus be classified as a protein with a moonlighting role in RhoA-dependent invasion. The uncoupling between invasive function and catalysis suggested that invasion may be mediated by protein−protein interactions. Consistent with this hypothesis, MRDI was found localized at the leading edge of cells, overlapping N-WASP and the site of actin polymerization, where its higher effective concentration might enable protein−protein interactions important for cell movement.

Interestingly, a protein originally characterized as an Apaf1 interacting protein that prevents hypoxia-induced apoptosis[7] was recently identified as MTRu-1-P dehydratase, the next enzyme in the methionine salvage pathway following MTR-1-P isomerase.[8,9] These recent findings further illustrate the prevalence of dual roles in metabolic enzymes and suggest that protein−protein interactions may be a general, catalysis-independent mechanism for their moonlighting functions.

Here, we examined MRDI by X-ray crystallography to analyze the structural basis for its dual function. The X-ray structure of the human protein solved to 2.5 Å reveals similarities to previous structures of bacterial and yeast MTR-1-P isomerases, with conserved residues found within an open conformation of the active site. Expression of the bacterial enzyme in human cells depleted for MRDI enabled rescue of cell growth in the presence of MTA, but not cell invasion in collagen spheroids. Mutation of amino acids within a putative binding pocket unique to human MRDI resulted in inhibition of spheroid invasion. Together the results indicate that the dual function of MRDI can be attributed to distinct protein regions, including a conserved catalytic site which is needed for metabolic activity, and a separate binding pocket, distal to the active site, which is responsible for RhoA-dependent cell invasion.

MATERIALS AND METHODS

Cloning and Mutagenesis. Cloning, heterologous expression in *Escherichia coli*, and purification of MRDI were carried out as described.[4] The human MRDI gene containing silent mutations to bypass the shRNA interference (bpWT) was subcloned into the plasmid pET41b+ for *E. coli* expression. This plasmid was then used to introduce all of the point mutations used in this study, using the QuikChange (Invitrogen) site-directed mutagenesis protocol, using the mutagenic primers shown in Supplemental Table ST1 in the Supporting Information. The mutations were confirmed by sequencing and subcloned, using *Not*I and *Sfi*I restriction sites, into the pREX-MRDI bpWT plasmid[4] for retroviral expression in A375 cells. The genes for *Bacillus subtilis* MtnA and *Saccharomyces cerevisiae* Ypr118W were PCR-amplified from genomic DNA using the primers shown in Supplemental Table ST1. The C-terminal primers incorporated a hemagglutinin (HA) fusion tag at the C-termini of both genes. The amplified fragments were digested with *Eco*RI and *Not*I and ligated into the pREX vector digested with the same restriction enzymes. The correctness of the final products was confirmed by DNA sequencing.

Protein Crystallization and X-ray Data Collection. Crystals of MRDI were grown in hanging drops at 16 °C in a precipitant solution containing 0.7 M sodium citrate and 100 mM imidazole, pH 8.0. Crystals appeared overnight, but growth was allowed to continue for 1 week, after which no additional growth was observed. For data collection, crystals were transferred to a cryoprotecting solution composed of 10% glycerol, 0.7 M sodium citrate, and 100 mM imidazole, pH 8.0, and flash-frozen in a nitrogen stream at 100 K. Diffraction data were collected with a rotating anode generator using Cu Kα radiation and a Rigaku R-AXIS IV++ image plate detector placed such that the direct beam was centered on the detector (no detector swing). The crystal to detector distance was set at 200 mm and 130° of data collected in 0.5° oscillations. The crystals belonged to space group $P2_12_12_1$, with unit cell dimensions a = 44.8, b = 116.5, c = 137.9 Å, and $\alpha = \beta = \gamma = 90°$.

Crystals of MRDI Ser283Tyr were grown under conditions similar to those of the wild type protein. The crystals were frozen as described above and diffraction data collected at beamline 5.0.2 of the Advanced Light Source, Lawrence Berkeley National Laboratories. Radiation wavelength was set to 1 Å, and an ADSC CCD detector was placed 250 mm from the crystal (no detector swing). Analysis of preliminary diffraction images with Mosflm[10,11] confirmed that the lattice of the mutant protein crystal was similar to that of the wild type and allowed development of a collection strategy to maximize data completeness and redundancy while minimizing total exposure. On the basis of these estimates, 100° of data were collected in 1° oscillations. Data reduction for both crystals was carried out in HKL2000,[12] and data collection statistics are summarized in Table 1.

Structure Determination and Refinement. A sequence similarity search of the Protein Data Bank using BLAST revealed a protein annotated eIF2B from *Leishmania major* (PDB ID 2A0U, J. Bosch and W. Hol, unpublished results) sharing 45% sequence identity with MRDI, suggesting that this protein could be used as a model to determine the MRDI structure by molecular replacement. To maximize the similarity between the model and MRDI, we used the program CHAINSAW[13] to prune nonconserved residues to the gamma carbon while conserved residues were left intact. The *Leishmania* protein was a dimer in the crystallographic asymmetric unit. We used the dimer as a search model, as analysis of the MRDI crystal lattice contents suggested the presence of two monomers per asymmetric unit. Rotation/translation searches with the program Phaser[14] using data to 2.5 Å resolution yielded a clear solution without significant packing clashes. Using the program CNS,[15] the model was subjected to one round of refinement, and an electron density map was calculated to 2.5 Å resolution. Several amino acid side chains missing from the model were readily observed in the electron density map, validating the correctness of the molecular replacement solution. The model was rebuilt using the programs O[16] and Coot,[17] and alternative rounds of refinement and rebuilding were performed until no further improvement of the R factors was achieved. The structure of MRDI Ser283Tyr was determined using the MRDI structure as a starting model, where Ser283 was mutated to Ala, all water molecules were removed, and all B factors were randomized. The model was then subjected to rigid body refinement followed by rebuilding and positional and B factor refinement in PHENIX.[18] Final refinement statistics are summarized in Table 1.

Table 1. Data Collection and Refinement Statistics[a]

data collection statistics	wild type	S283Y
wavelength (Å)	1.54	1.00
space group	$P2_12_12_1$	$P2_12_12_1$
cell dimensions (Å)	a = 44.8, b = 116.6, c = 136.9 $\alpha = \beta = \gamma = 90°$	a = 44.5, b = 116.0, c = 135.5 $\alpha = \beta = \gamma = 90°$
resolution (Å)	30.00 − 2.50 (2.59 − 2.50)	100.0 − 2.30 (2.34 − 2.30)
unique reflections	25424 (2463)	32169 (1576)
I/σ	27.2 (5.3)	22.1 (3.0)
Wilson B factor	36.33	34.80
redundancy	4.3 (4.1)	3.9 (3.8)
data completeness (%)	99.2 (98.7)	99.4 (98.5)
R_{merge} (%)	8.0 (35.9)	6.5 (41.6)
refinement statistics		
R_{work} (%)	17.9 (19.6)	18.0 (20.8)
R_{free} (%)	21.1 (25.7)	20.8 (24.6)
no. of non-H protein atoms	5282	5294
no. of water atoms	162	313
no. of amino acid residues	709	709
mean B value (Å^2)	33.6	34.0
mean B value protein (Å^2)	33.9	34.0
mean B value solvent molecules (Å^2)	26.6	34.3
rms deviation from ideal values		
bond lengths (Å)	0.006	0.005
bond angles (deg)	1.06	0.96
residues in Ramachandran plot		
most favored regions (%)	97.4	97.0
generously allowed regions (%)	2.3	2.7
outliers (%)	0.3	0.3

[a]Values in parentheses represent the highest resolution shell.

Cell Culture and Western Blotting. A375 melanoma cell lines were obtained from ATCC and maintained in 10% FBS−RPMI. Cells with stable shRNA knockdown of MRDI were treated to stably express WT or mutant MRDI or the MTR-1-P isomerase, (HA tagged)-MtnA from *B. subtilis*, using retroviral delivery as described.[4] Expression was confirmed by Western blotting using anti-MRDI polyclonal antibodies obtained by immunization of rabbits with a synthetic peptide corresponding to amino acids 356−369 of human MRDI (TISSRDGTLDGPQM; Sigma-Genosys), or rabbit anti-HA antibodies (HA.11, Covance) as primary antibodies. Secondary anti-rabbit or anti-mouse antibodies coupled to horseradish peroxidase (Jackson ImmunoResearch Laboratories) and enhanced chemiluminescence substrates (Amersham) recorded on film were then used to visualize immunoreactive bands.

Cell Proliferation and Invasion Assays. Assays for rescue of cell viability by MTR-1-P isomerase expression were conducted by plating cells in duplicate into 6-well chambers (100 000 cells/well) with 3 mL of RPMI + 10% FBS. After overnight incubation to allow cell adhesion, the medium was replaced with 3 mL of methionine-free RPMI + 10% dialyzed FBS, supplemented with or without methylthioadenosine (30 μM) or methionine (15 mg/mL). After 96 h, cells were trypsinized and counted in trypan blue using a hemocytometer. Cell counts were obtained by averaging values from four replicate measurements made from each of the duplicate wells. Spheroid cell invasion assays were carried out as described.[19,20] Briefly, 25 000 melanoma cells were plated in triplicate into 6-well plates containing 1.5% Noble agar, in RPMI-10% FBS. After 3−5 days, spheroids were collected by centrifugation, resuspended into 2.5 mg/mL collagen, and overlaid on a presolidified layer of the same collagen solution. Images of spheroids were collected 4 days after implantation, using an Olympus IX81 microscope equipped with a DP70-CCD camera for phase microscopy. Spheroid growth was quantified by measuring the diameter of the inner core of cells (in mm), and cell invasion measured the outer radius of cells invading into collagen minus the inner radius. For each spheroid, the radii along four to eight axes were measured and averaged.

RESULTS

Distinct Properties of MTR-1-P Isomerases from Humans and Bacteria. Our previous study established the catalytic activity of MRDI as an MTR-1-P isomerase.[3] Deletion of MRDI from human cells or mutation of conserved residues Cys168 or Asp248 abolished the ability of human cells to grow in methionine-free media supplemented with MTA as a source of methionine produced by the salvage pathway. Orthologous MTR-1-P isomerases have been reported to function in methionine salvage.[21,22] *B. subtilis* MtnA shares 39% sequence identity with MRDI (Supplementary Figure S1). Its MTR-1-P isomerase activity has been verified in vitro, and its structure in complex with product MTRu-1-P has been reported.[22]

To test whether *B. subtilis* MtnA was able to substitute for MRDI in human cells with respect to methionine salvage and/or invasion, we stably expressed HA-tagged MtnA in melanoma cells that were depleted of MRDI using shRNA. MtnA expression had little effect on cells growing in complete media (Figure 1A). However, whereas cells depleted of MRDI started to die after 48 h in methionine-free media supplemented with MTA, expression of MtnA in these cells supported continued growth to approximately 90% of the wild type cell levels (Figure 1B). This indicates that the bacterial orthologue rescues the loss of MRDI with respect to its methionine salvage function. By comparison, overexpression of an MRDI variant containing silent cDNA mutations, which bypasses shRNA but yields a WT protein sequence (bpWT), supported more robust growth in methionine-free media containing MTA, to approximately 200% of wild type levels.

To test whether MtnA could also support the cell invasion phenotype, cells depleted of MRDI and expressing MtnA were grown as 3D spheroids implanted into collagen. MtnA failed to increase cell invasion over levels observed in MRDI-depleted cells (Figure 1C,D), whereas expression of recombinant MRDI-bpWT readily reversed the invasion phenotype. Thus, the bacterial orthologue shared MRDI's function as a metabolic enzyme, but lacked its function as a mediator of cell invasion.

Crystal Structure of Human MRDI. To better understand the unique features that distinguish MRDI from the bacterial MTR-1-P isomerase, the protein was crystallized and its 3D structure determined (Figure 2A). As detailed under Materials and Methods, the structure was determined by molecular replacement using a homologous structure from *L. major* (PDB ID 2A0U, J. Bosch and W. Hol, unpublished results) as the search model and refined to 2.5 Å resolution. MRDI is a dimer in solution as determined by size exclusion chromatog-

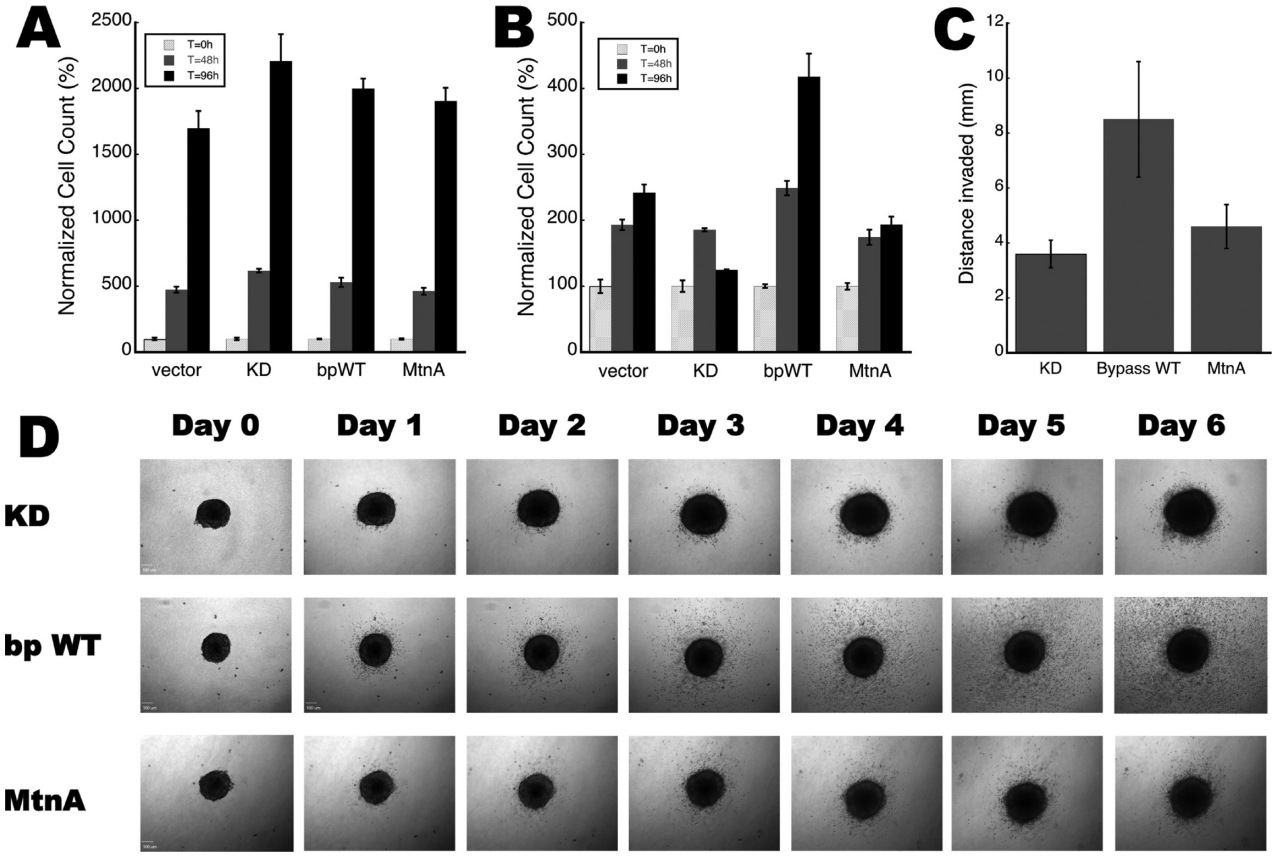

Figure 1. Phenotypes of MRDI and MtnA expression and deletion. (A) Growth in full media of A375 melanoma cells, carrying empty vector (Vector), depleted of MRDI with shRNA (KD), depleted of endogenous MRDI and expressing a wild-type bypass MRDI (bpWT), or depleted of endogenous MRDI and expressing *B. subtilis* MtnA (MtnA). The bars represent cell counts for time 0, 48, and 96 h normalized to that of cells carrying empty vector at time 0 h. (B) Same as (A) but with cells grown in methionine-free media supplemented with 30 μM MTA. (C) Quantitation of cell invasiveness in 3D spheroid assays carried out as described under Materials and Methods. Values represent the mean of 10−11 independent experiments. The error bars represent standard deviation of the mean. (D) Representative images of 3D spheroid invasion assays, for cells quantified in (C).

raphy (data not shown), and the crystallographic asymmetric unit contains one MRDI dimer. The final model contains all residues except the N-terminal methionine in each subunit and the last 15 amino acids (the last 12 on chain B), presumably due to conformational flexibility. The final model had an R value = 0.178 and R_{free} = 0.211 with excellent stereochemistry and 97.4% of nonglycine residues in the most favored regions of the Ramachandran plot. Two flexible loops in the N-terminus (residues 66−72 and 113−117) display high B factors (Figure 2B). Leu72 residues lie within the 66−72 loop of each chain and represent the only two residues that refine as Ramachandran outliers, likely due to conformational flexibility. Data collection and refinement statistics are summarized in Table 1, and a representative piece of the electron density is shown in Supplementary Figure S2.

The individual subunits have essentially identical conformations, with RMSD = 0.5 Å for all 353 Cα atoms common to both protomers. Each monomer contains two distinct domains. The N-terminal domain is arranged in a five-helix bundle and a three-stranded β-sheet (red and blue, Figure 2A), whereas the C-terminal domain forms a Rossmann-like fold (orange and green, Figure 2A) and includes a dimerization interface, which buries approximately 4720 Å^2 of surface area. A long α-helix provides the connection between the two domains (Figure 2A). The N-terminal domains of both chains have higher temperature factors than the C-terminal domains, possibly reflecting flexibility on the connecting α-helix (Figure 2B). A deep cleft between N- and C-terminal domains forms the active site containing catalytic residues Cys168 and Asp248 (Figure 2A, shown as space-filling models). Sequence alignment revealed strong conservation of the residues lining the active site cleft but significant divergence among the surface-exposed residues (Figure 2C,D).

Open-Closed Conformational Change in MTR-1-P Isomerases. The structure of MtnA was determined with the MTRu-1-P product bound in its active site.[22] Comparison of this structure to MRDI reveals a striking conformational difference, where the N-terminal domain of MtnA is rotated approximately 30° (estimated with Dyn Dom[23]) and collapsed on top of the C-terminal domain, closing the active site cleft around the ligand (Figure 3A,B). Therefore, MRDI adopts an open conformation of the enzyme, whereas MtnA in complex with MTRu-1-P adopts a closed conformation, as previously hypothesized by Tamura et al.[22] To test the feasibility of this conformational change, we separated the N- and C-terminal domains of MtnA and superimposed them independently onto the N- and C-terminal domains of MRDI. The results showed excellent agreement between the two structures, without significant clashes. Similarly, the N- and C-terminal domains could be superimposed onto the MtnA structure without major clashes, suggesting that an open-to-closed transition is feasible in these MTR-1-P isomerases. The apparent flexibility of the α-helix that connects the N- and C-terminal domains (Figure 2B) is also consistent with this conformational change as the transition is mediated by bending of this α-helix.

dx.doi.org/10.1021/bi400556e | *Biochemistry* 2013, 52, 5675−5684

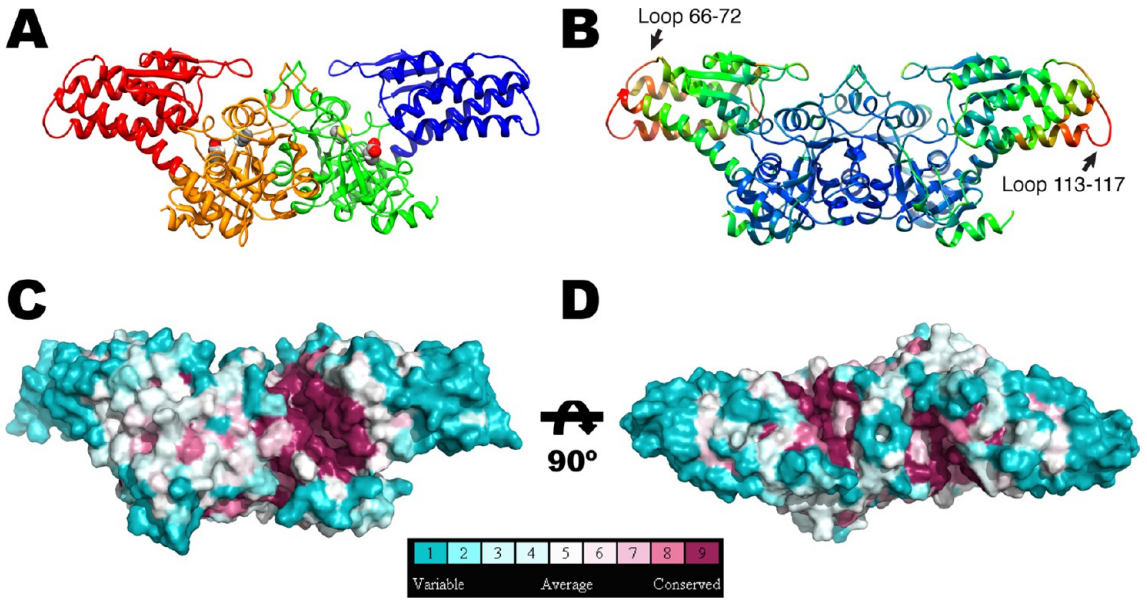

Figure 2. X-ray structure of MRDI. (A) "Side" view of the MRDI dimer, with N-terminal domains colored red and blue and C-terminal domains colored orange and green. The side chains of catalytically important residues Cys 168 and Asp248 are highlighted as space filling models, with sulfur atoms indicated in yellow and oxygen atoms in red. A long α-helix connecting the N- and C-terminal domains is indicated with arrows. (B) "Side" view of the MRDI dimer, colored by the average *B* factor going from blue (low *B* factor) to red (high *B* factor). Note the higher temperature factors in both N-terminal domains, suggesting flexibility in the connecting helix. Flexible loops at the tips of the N-terminal domains are labeled with their amino acid numbers. (C, D) Side and top views of the MRDI dimer, where sequence conservation is mapped to the surface. The amino acid conservation was analyzed with the Consurf server, where the rapidly evolving (variable) positions are colored dark cyan, positions with average variability are colored white, and slowly evolving (conserved) positions are colored dark purple.

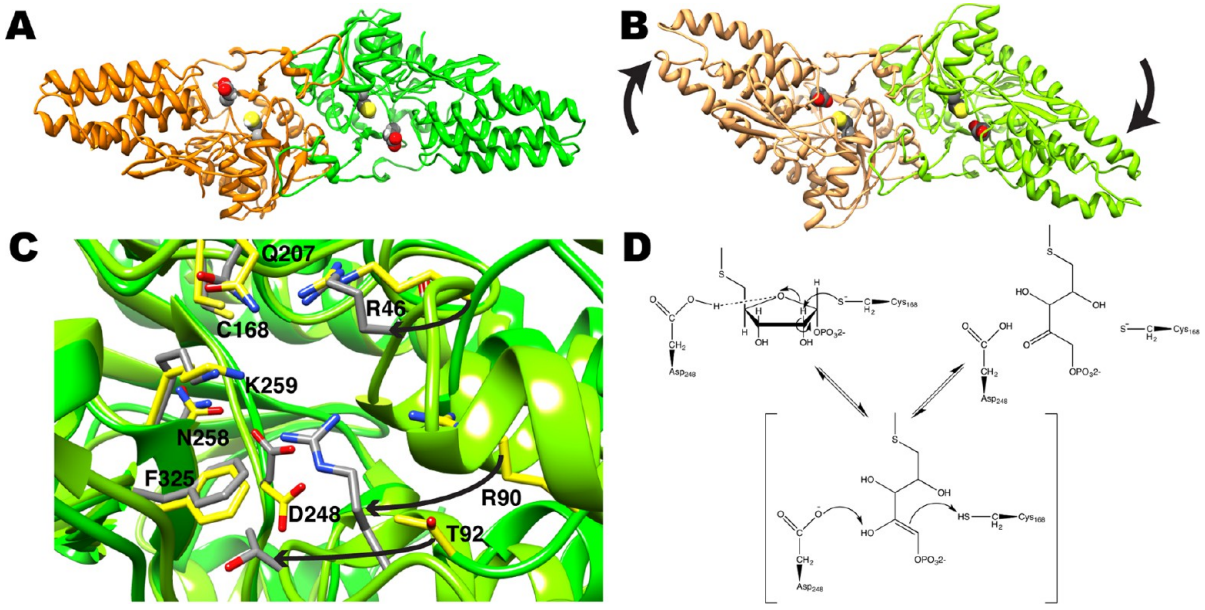

Figure 3. Open-closed conformations in MTR-1-P isomerases. Top views of (A) MRDI apo form and (B) MtnA−MTRu-1-P cocrystal. Each subunit within the dimers are colored in shades of orange and green. The catalytically important Cys and Asp resides are highlighted as space-filling models. The curved arrows indicate the conformational change that the N-terminal domains would trace, in going from the open conformation, illustrated by MRDI (A), to the closed conformation illustrated by MTRu-1-P bound MtnA (B). (C) Close up view of the active site residues in a superposition of MRDI (dark green backbone and yellow side chains) in the open conformation and MtnA (light green backbone and gray side chains) in the closed conformation. The displacement of residues in the N-terminal domain that participate in ligand binding is highlighted with arrows. (D) Proposed catalytic mechanism for the isomerization reaction catalyzed by MRDI.

In addition to the catalytic residues Cys168 and Asp248, all residues that were identified in MtnA as important for ligand binding[24] were strictly conserved in MRDI. These included Arg46−Pro49 and Arg90−Thr92 in the N-terminal domain and Ala174, Thr175, Gln207, Asn258, Lys259, and Phe325 in the C-terminal domain. Figure 3C shows a superposition of the conserved active site residues in MRDI (dark green) and ligand-bound MtnA (light green and gray side chains), which illustrates the rearrangement of the N-terminal domain ligand binding residues (Arg46, Arg90, and Thr92) due to the open-to-closed

dx.doi.org/10.1021/bi400556e | *Biochemistry* 2013, 52, 5675−5684

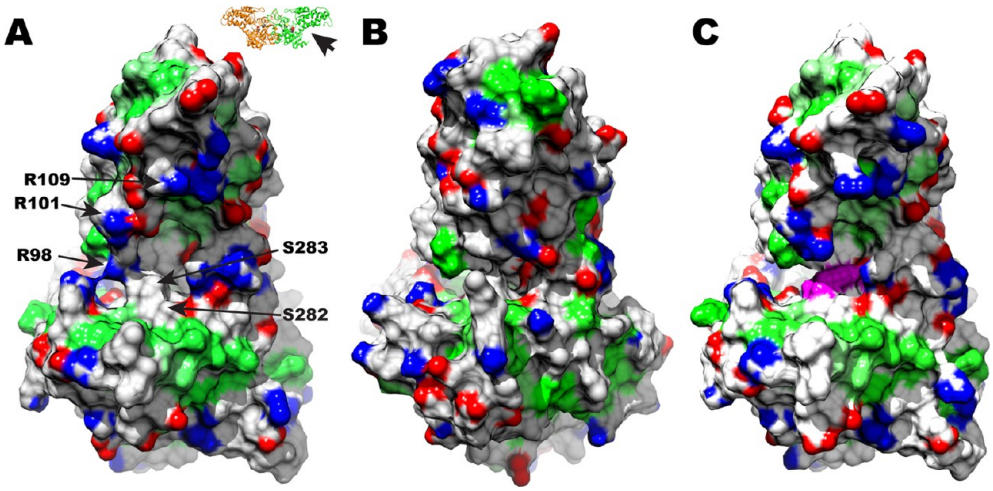

Figure 4. Surface features of MRDI and MtnA. Surface representation of (A) MRDI, (B) MtnA, and (C) MRDI-Ser283Tyr, viewed from the side that is indicated in the inset by a black arrow. Nitrogen atoms on Arg, Lys, and His side chains are colored blue. Oxygen atoms on Glu and Asp side chains are colored red. Amino acids were assigned a hydrophobicity value according to the Kyte−Doolittle scale[36] and colored from bright green for the most hydrophobic residues (Ile, 4.5) to white for residues with score less than or equal to 0 (Gly, −0.4; Arg, −4.5). Residues selected for mutation are labeled as in (A). The side chain of Tyr283 is highlighted in magenta in (C).

transition. A possible reaction mechanism for the isomerization reaction is shown in Figure 3D. In this scheme, the deprotonated side chain of Cys168 abstracts a proton from C2, whereas Asp248 donates a proton to the furanose oxygen to promote ring-opening with formation of a double bond between C1 and C2. Proton transfer from the O2 of the enediol intermediate to Asp248 and from the protonated side chain of Cys168 to C1 forms the product MTRu-1-P and regenerates the initial state of the enzyme. A similar mechanism was proposed by Tamura and co-workers, although an additional hydride transfer alternative was also proposed.[22]

Divergent Features in MRDI Identify a Potential Binding Site Controlling Invasion. In MRDI, the isomerase catalytic function is uncoupled from the invasion function, as demonstrated by the ability of catalytically inactive MRDI mutants to support invasion. Given that MtnA was also unable to support the invasion phenotype (Figure 1C), we speculated that the invasion function might involve protein−protein interactions within regions distinct from the catalytic site, which is also the region showing highest conservation of surface residues (Figure 2C,D). MRDI was thus inspected for surface residues that were not conserved between the two isomerases, as well as surface features unique to MRDI, to identify potential binding regions for protein effectors of invasion. Comparison of the surface features of MRDI and MtnA modeled in the open conformation (most similar to MRDI) identified a distinctive cavity in MRDI, located on the concave face opposite the active site cleft, lined with a patch of surface exposed hydrophobic residues (Figure 4A; Supplementary Movie 1). In contrast, the corresponding surface in MtnA was shallower and lined with charged residues (Figure 4B; Supplementary Movie 2).

To test the importance of this surface, single mutations to Ala were introduced, replacing nonconserved residues Arg98, Arg101, and Arg109 in MRDI. In addition, Glu and Trp mutations of Ser282 and Tyr mutations of Ser283, located in the center of this pocket, were constructed with the hypothesis that larger side chains might disrupt potential binding to this interface. Modeling of the mutant side chains on MRDI showed that multiple common rotamers could be accommodated without clashes. Therefore, the mutations were not expected to interfere with the correct folding of MRDI.

WT and mutant MRDI cDNA were stably expressed in cells depleted for endogenous MRDI by shRNA knockdown, and cells were assayed for spheroid invasion in collagen. Little or no difference was observed between expression of bpWT MRDI and the mutants with respect to the ability of cells to proliferate, as measured by the spheroid growth. However, when collagen cell invasion was quantified by the difference between the outer radius representing the furthest extent of cell migration and the inner radius of the compacted spheroid, MRDI mutants Arg109Ala and Ser283Tyr showed suppression (Figure 5A,B), comparable to the levels observed in the MRDI shRNA knockdown condition. Western blotting confirmed that the expression levels of all MRDI mutants were comparable to the expression of bpWT (Figure 5C). In addition, we determined the crystal structure of MRDI-Ser283Tyr to rigorously rule out the possibility that impaired invasion might be caused by folding defects introduced by the Ser283Tyr mutation. The mutant structure was essentially identical to that of WT-MRDI, with an RMSD of 0.2 Å for all 356 Cα carbons. The only significant difference was the expected protuberance produced by the large tyrosine side chain within the cavity (Figure 4C; Supplementary Movie 3). Hence, rescue of invasion could be blocked by a mutation in MRDI (Ser283Tyr) that disrupted the geometry of the proposed binding pocket and another mutation (Arg109Ala) that removed a basic surface charge. We propose that these mutations define a binding pocket which functions to mediate interactions between MRDI and as yet unknown cellular effectors of invasion.

■ DISCUSSION

MRDI was initially identified as a gene product elevated in response to constitutively activated RhoA-GTP in cell lines derived from human melanoma metastases.[4] MRDI regulates tyrosine phosphorylation of focal adhesion kinase and modulates cell invasion in melanoma cells, and for this reason it was named "mediator of RhoA-dependent invasion (MRDI)". On the basis of its similarity with known isomerases, MRDI was shown to catalyze the conversion of MTR-1-P to MTRu-1-P, an important

dx.doi.org/10.1021/bi400556e | *Biochemistry* 2013, 52, 5675−5684

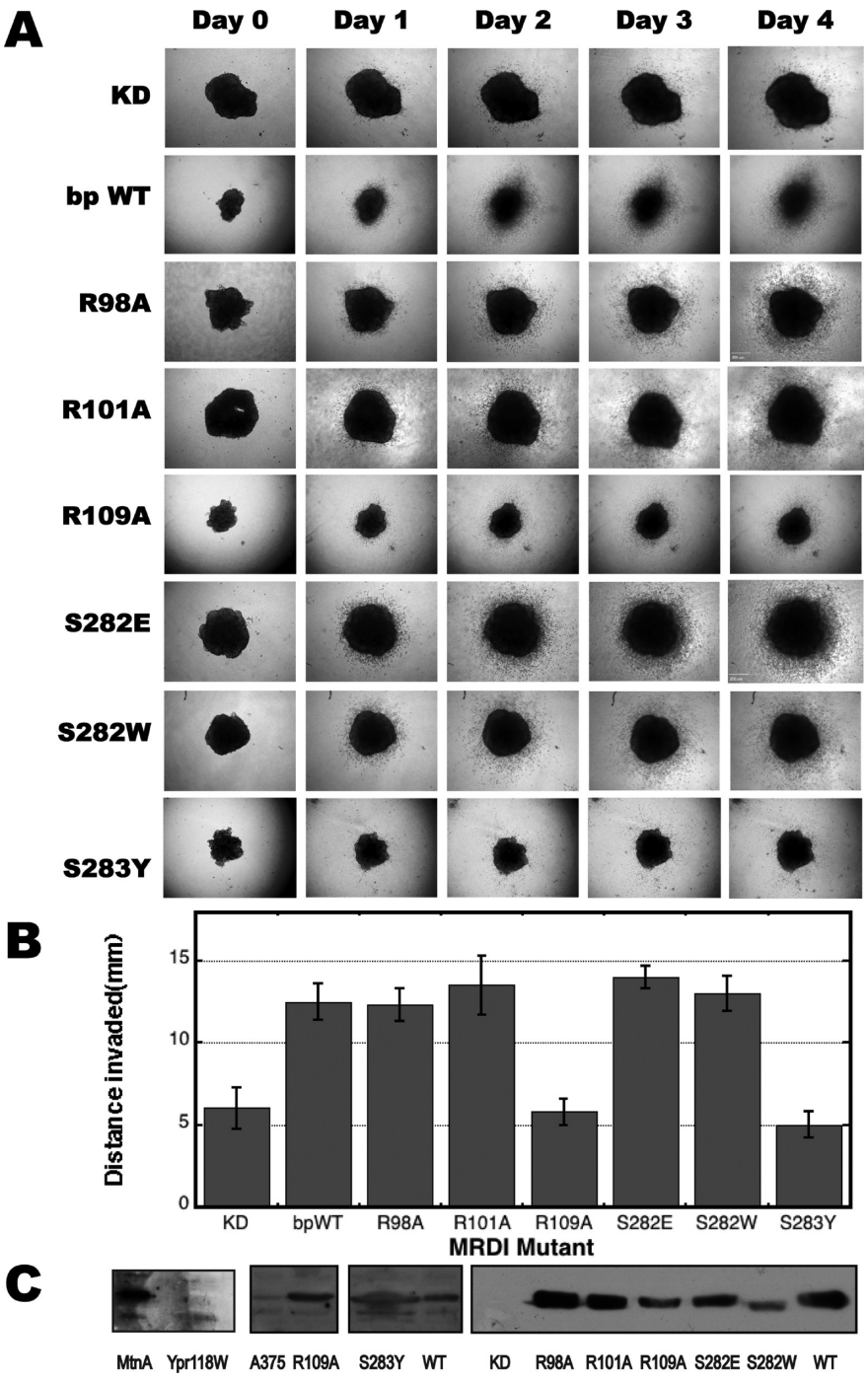

Figure 5. 3D spheroid cell invasion assay for MRDI mutants. (A) Representative images of spheroids after 0−4 days in A375 cells depleted of endogenous MRDI with shRNA (KD), depleted of MRDI and expressing WT-MRDI (bpWT), and depleted of MRDI and expressing MRDI mutants (mutations indicated). (B) Extent of cell invasion into collagen, quantified as described under Materials and Methods. Values represent the mean of four to eight independent experiments. The error bars represent standard error of the mean. (C) Western blots using anti-MRDI antibodies of naïve A375 cells (A375), A375 cells depleted of endogenous MRDI with shRNA (KD), KD and expressing MRDI bypass wild type mutant (bpWT), or KD and expressing the indicated MRDI mutants. The left panel shows a Western blot developed using anti-HA antibody of A375 cells depleted of endogenous MRDI and expressing HA-tagged *B. subtilis* MtnA or *S. cerevisiae* Ypr118W. Because expression of Ypr118W was poor, it was excluded from analysis.

reaction in the methionine salvage pathway. Consistent with this role, MRDI was required for cells to grow in methionine-free media supplemented with MTA, the metabolic precursor to MTR-1-P that is eventually converted to methionine. Mutation of residues Cys168 and Asp248 abolished MRDI's isomerase activity and its ability to support growth in methionine-free, MTA-supplemented media. However, its ability to mediate the invasion phenotype in melanoma-derived cell was unaffected. This indicated that the "moonlighting" role of MRDI as a regulator of cell invasion evolved from a protein with enzymatic function in amino acid metabolism.

Our work defines the structural features in MRDI that mediate its distinct function in invasion. The structure of MRDI shows a high degree of similarity with known MTR-1-P isomerases, such

dx.doi.org/10.1021/bi400556e | *Biochemistry* 2013, 52, 5675−5684

as *B. subtilis* MtnA and *S. cerevisiae* Ypr118w.[21,22] These dimeric proteins have N- and C-terminal domains linked through a long α-helix and an active site cleft defined by the interface between the two domains. MtnA rescued methionine salvage in cells depleted of MRDI by shRNA, indicating that the isomerase function in methionine salvage appears ancient. (Analogous rescue experiments could not be conducted with yeast Ypr118W because the protein expressed poorly in A375 cells (Figure 5C)). This is consistent with the MRDI structure, which showed high conservation of not only the catalytic residues but also the residues lining the entire active site cleft (Figures 2C,D and 3C). However, despite structural similarity with MRDI, MtnA when expressed in A375 melanoma cells was incapable of supporting the invasion phenotype (Figure 1). Therefore, we conclude that the invasion phenotype is unrelated to the conserved active site residue and unique to the human MRDI.

Comparison of the MRDI structure with that of product (MTRu-1-P)-bound MtnA revealed two distinct conformations, consistent with a proposed domain closure in MTR-1-P isomerases.[22] Ligand-free MRDI represents an open conformation, where the active site cleft is solvent exposed. Conversely, product-bound MtnA represents a closed conformation, where the N- and C-terminal domains collapse around the ligand, closing the active site cleft (Figure 3A−C). Interestingly, the structure reported for apo-MtnA also formed a closed conformation in the absence of ligand.[22] However, this protein was crystallized from ammonium sulfate, and a sulfate ion was found in the same position occupied by the phosphate from MTRu-1-P in the liganded structure. Similarly, the yeast orthologue Ypr118w was also crystallized from ammonium sulfate, and the structure formed the closed conformation containing a sulfate ion in the active site.[21] This suggests that coordination of the substrate phosphate (or sulfate at high concentrations) is enough to induce domain closure.

MTR-1-P isomerases including MRDI are part of a superfamily related by sequence to α, β, and δ subunits of the eukaryotic translation initiation factor 2B (eIF2B). eIF2B is a heteropentameric complex, which functions as the guanine nucleotide exchange factor (GEF) for the G-protein "eukaryotic initiator factor 2" (eIF2) and promotes translational initiation.[5,25] However, the GEF activity of eIF2B depends on its catalytic $\gamma-\varepsilon$ subunits, whereas the roles of the α, β, and δ subunits are unclear but appear to modulate the activity of the catalytic subunits. In the structure of eIF2Bα, Hiyama and coworkers described a deep basic pocket at the interface between the N- and C-terminal domains.[26] The authors propose that this pocket represents a docking site for a phosphate group, which allows eIF2B to recognize eIF2α phosphorylated at Ser51[27] by various upstream kinases, such as GCN2, PERK, PKR, and HRI. Analogous to the structures of *S. cerevisiae* Ypr118w and *B. subtilis* MtnA, the structure of eIF2Bα was solved with a sulfate ion cocrystallized in this basic pocket. eIF2Bα residues coordinating the sulfate ion were Arg108, Ser131, Arg132, Ala197, Asp208, and Glu231. If MRDI were a viable subunit substitute for eIF2B subunits, we would expect these residues to be conserved. However, a structure-based sequence alignment of MRDI with eIF2Bα performed with Dali[28] shows that only the residues corresponding to Ala197 and Asp 208 in MRDI were conserved. Thus, it is unlikely that the moonlighting invasion function of MRDI is associated with a role in translational initiation. An alternative possibility is that phosphorylated effector proteins might be recognized by the negatively charged active site groove in MRDI, analogous to the recognition of phospho-eIF2 by eIF2B. However, this would have predicted that MtnA, which retained the negatively charged active site groove, should have supported the invasion phenotype, which was not observed.

Therefore, MRDI is part of an evolutionary progression that connects protein synthesis, amino acid metabolism, and signal transduction. Structurally, MRDI and MtnA are part of the eIF2B superfamily, but they are functionally distinct from the translational regulators and instead share MTR-1-P isomerase activity. The human MRDI represents a new branch distinct from bacterial and yeast orthologues, by acquiring a unique function in signal-dependent cell invasion.

We considered whether the role of MRDI in invasion might involve a separate region involving nonconserved surface features unique to MRDI, which could, for example, serve as a binding site for interactions with other protein effectors. To facilitate the search for such structural features, we modeled MtnA in an open conformation similar to that of MRDI. A cavity unique to MRDI was identified, lined by a large hydrophobic patch on a concave surface, opposite each active site cleft in MRDI (Figure 4). Given that protein−protein interaction interfaces are typically enriched in hydrophobic residues,[29] we tested the possibility that this interface might be associated with the unique invasive function of MRDI. If our hypothesis were correct, we expected that replacing a small side chain with a large bulky residue would have a dramatic effect on blocking binding interactions, due to steric hindrance. Consistent with this hypothesis, the Ser283Tyr mutation introduced a large protuberance in the concave surface (Figure 4C), coupled to an inability to rescue invasion (Figure 5). On the other hand, Ser282Trp and Ser282Glu had no effect on the invasion phenotype. However, modeling indicated that some allowed rotamers of these mutants would have little impact on the interface geometry.

We also tested the importance of specific surface-exposed residues that were also unique to MRDI. Mutation of nonconserved Arg residues revealed the importance of Arg109 in invasion. Taken together, these results support the conclusion that the invasion phenotype is independent of catalysis and may instead be controlled by interactions between MRDI and other proteins through sites on the dimer outside the active sites.

There is precedent for enzymes evolving moonlighting functions that require binding sites distal from the active site. For example, *Hansenula polymorpha* pyruvate carboxylase was shown to moonlight as an assembly factor for alcohol oxidase and mediate its import into the peroxisome.[30] Whereas the active site of pyruvate carboxylase is located at the C-terminal side of the β-strands that make up its TIM barrel structure, the residues required for the moonlighting activity are clustered on the opposite, N-terminal, side of the β-strands in the TIM barrel.[30] Proteins without catalytic activities can also develop moonlighting roles involving distinct binding sites in the protein. One such case is illustrated by tumor necrosis factor, the receptor-binding domain of which promotes an inflammatory response. However, residues distant from the receptor binding site that map to the lectin-like domain mediate noncytokine effects of tumor necrosis factor, such as lysis of trypanosomes[31] and protection against pulmonary edema.[32,33] It is fascinating that MTRu-1-P dehydratase, the next enzyme following MRDI in the methionine salvage pathway, also has a moonlighting function as an antiapoptotic protein through its Apaf-1 binding activity.[8,9] MTA phosphorylase, the enzyme immediately preceding MRDI in methionine salvage, also functions as a tumor suppressor gene, although it is possible that this may be due to its enzymatic role in methionine salvage, by depleting cellular levels of MTA.[34] Our

findings, which now map the catalytic and invasion-related functions of MRDI to distinct regions of the structure, contribute to the growing evidence that moonlighting proteins have greater prevalence as well as an expanded importance in cell physiology than initially appreciated.[1,35]

■ ASSOCIATED CONTENT

Supporting Information

Sequence alignment of MRDI, *B. subtilis* MtnA and *S. cerevisiae* Ypr118w (Figure S1); representative sample of the elctron density map associated with the final MRDI model (Figure S2); table with primers used for cloning and mutagenesis; and three movies highlighting the surface features of MRDI and MtnA. This material is available free of charge via the Internet at http://pubs.acs.org.

Accession Codes

Coordinate and structure factors for MRDI and MRDI_S283Y have been deposited in the Protein Databank with IDs 4LDQ and 4LDR, respectively.

■ AUTHOR INFORMATION

Corresponding Author

*(N.G.A.) Mailing address: Department of Chemistry and Biochemistry, University of Colorado at Boulder, Boulder, CO 80309-0596, USA. Phone: (303) 492-4799. E-mail: natalie.ahn@colorado.edu. (M.C.S.) Mailing address: Department of Chemistry and Biochemistry, University of Colorado at Boulder, Boulder, CO 80309-0596, USA. Phone: (303) 735-4341. E-mail: marcelo.sousa@colorado.edu.

Funding

This work was supported by NIH Grants R01 CA118972 (N.G.A.) and T32 GM008759 (P.D.T.). Structural biology research at the University of Colorado, Boulder, is supported in part by the William M. Keck Foundation. Part of the work presented in this paper was carried out at The Advanced Light Source, which is supported by the Director, Office of Science, Office of Basic Energy Sciences, of the U.S. Department of Energy under Contract DE-AC02-05CH11231.

Notes

The authors declare no competing financial interest.

■ ACKNOWLEDGMENTS

We are indebted to Theresa Nahreini for assistance with cell culture and to Steven Edwards and David McKay for X-ray facility support.

■ ABBREVIATIONS USED

MRDI, mediator of RhoA-dependent invasion; MTR-1-P, methylthioribose-1-phosphate; MTRu-1-P, methylthioribulose-1-phosphate; MTA, methylthioadenosine; KD, knockdown; bpWT, wild-type MRDI containing silent mutations which bypass shRNA; eIF2B, eukaryotic initiation Factor 2B; HA, hemagglutinin; FBS, fetal bovine serum

■ REFERENCES

(1) Copley, S. D. (2012) Moonlighting is mainstream: paradigm adjustment required. *Bioessays 34*, 578−588.

(2) Jeffery, C. J. (2003) Moonlighting proteins: old proteins learning new tricks. *Trends Genet. 19*, 415−417.

(3) Rouault, T. A. (2006) The role of iron regulatory proteins in mammalian iron homeostasis and disease. *Nat. Chem. Biol. 2*, 406−414.

(4) Kabuyama, Y., Litman, E. S., Templeton, P. D., Metzner, S. I., Witze, E. S., Argast, G. M., Langer, S. J., Polvinen, K., Shellman, Y., Chan, D., Shabb, J. B., Fitzpatrick, J. E., Resing, K. A., Sousa, M. C., and Ahn, N. G. (2009) A mediator of Rho-dependent invasion moonlights as a methionine salvage enzyme. *Mol. Cell Proteomics 8*, 2308−2320.

(5) Kyrpides, N. C., and Woese, C. R. (1998) Archaeal translation initiation revisited: the initiation factor 2 and eukaryotic initiation factor 2B alpha-beta-delta subunit families. *Proc. Natl. Acad. Sci. U.S.A. 95*, 3726−3730.

(6) Pirkov, I., Norbeck, J., Gustafsson, L., and Albers, E. (2008) A complete inventory of all enzymes in the eukaryotic methionine salvage pathway. *FEBS J. 275*, 4111−4120.

(7) Cho, D. H., Hong, Y. M., Lee, H. J., Woo, H. N., Pyo, J. O., Mak, T. W., and Jung, Y. K. (2004) Induced inhibition of ischemic/hypoxic injury by APIP, a novel Apaf-1-interacting protein. *J. Biol. Chem. 279*, 39942−39950.

(8) Ko, D. C., Gamazon, E. R., Shukla, K. P., Pfuetzner, R. A., Whittington, D., Holden, T. D., Brittnacher, M. J., Fong, C., Radey, M., Ogohara, C., Stark, A. L., Akey, J. M., Dolan, M. E., Wurfel, M. M., and Miller, S. I. (2012) Functional genetic screen of human diversity reveals that a methionine salvage enzyme regulates inflammatory cell death. *Proc. Natl. Acad. Sci. U.S.A. 109*, E2343−E2352.

(9) Mary, C., Duek, P., Salleron, L., Tienz, P., Bumann, D., Bairoch, A., and Lane, L. (2012) Functional identification of APIP as human mtnB, a key enzyme in the methionine salvage pathway. *PLoS One 7*, e52877.

(10) Battye, T. G., Kontogiannis, L., Johnson, O., Powell, H. R., and Leslie, A. G. (2011) iMOSFLM: a new graphical interface for diffraction-image processing with MOSFLM. *Acta Crystallogr. 67*, 271−281.

(11) Leslie, A. G. (2006) The integration of macromolecular diffraction data. *Acta Crystallogr. 62*, 48−57.

(12) Otwinowski, Z., and Minor, W. (1997) Processing of X-ray diffraction data collected in oscillation mode. *Methods Enzym. 276*, 307−326.

(13) Stein, N. (2008) CHAINSAW: a program for mutating pdb files used as templates in molecular replacement. *J. Appl. Crystallogr. 41*, 641−643.

(14) Mccoy, A. J., Grosse-Kunstleve, R. W., Adams, P. D., Winn, M. D., Storoni, L. C., and Read, R. J. (2007) Phaser crystallographic software. *J. Appl. Crystallogr. 40*, 658−674.

(15) Brünger, A. T., Adams, P. D., Clore, G. M., DeLano, W. L., Gros, P., Grosse-Kunstleve, R. W., Jiang, J. S., Kuszewski, J., Nilges, M., Pannu, N. S., Read, R. J., Rice, L. M., Simonson, T., and Warren, G. L. (1998) Crystallography & NMR system: a new software suite for macromolecular structure determination. *Acta Crystallogr. 54*, 905−921.

(16) Jones, A. (1978) A graphics model building and refinement system for macromolecules. *J. Appl. Crystallogr. 11*, 268−272.

(17) Emsley, P., and Cowtan, K. (2004) Coot: model-building tools for molecular graphics. *Acta Crystallogr. 60*, 2126−2132.

(18) Adams, P. D., Afonine, P. V., Bunkoczi, G., Chen, V. B., Davis, I. W., Echols, N., Headd, J. J., Hung, L. W., Kapral, G. J., Grosse-Kunstleve, R. W., McCoy, A. J., Moriarty, N. W., Oeffner, R., Read, R. J., Richardson, D. C., Richardson, J. S., Terwilliger, T. C., and Zwart, P. H. (2010) PHENIX: a comprehensive Python-based system for macromolecular structure solution. *Acta Crystallogr. 66*, 213−221.

(19) Argast, G. M., Croy, C. H., Couts, K. L., Zhang, Z., Litman, E., Chan, D. C., and Ahn, N. G. (2009) Plexin B1 is repressed by oncogenic B-Raf signaling and functions as a tumor suppressor in melanoma cells. *Oncogene 28*, 2697−2709.

(20) Smalley, K. S., Haass, N. K., Brafford, P. A., Lioni, M., Flaherty, K. T., and Herlyn, M. (2006) Multiple signaling pathways must be targeted to overcome drug resistance in cell lines derived from melanoma metastases. *Mol. Cancer Ther. 5*, 1136−1144.

(21) Bumann, M., Djafarzadeh, S., Oberholzer, A. E., Bigler, P., Altmann, M., Trachsel, H., and Baumann, U. (2004) Crystal structure of yeast Ypr118w, a methylthioribose-1-phosphate isomerase related to regulatory eIF2B subunits. *J. Biol. Chem. 279*, 37087−37094.

(22) Tamura, H., Saito, Y., Ashida, H., Inoue, T., Kai, Y., Yokota, A., and Matsumura, H. (2008) Crystal structure of 5-methylthioribose 1-

phosphate isomerase product complex from *Bacillus subtilis*: implications for catalytic mechanism. *Protein Sci. 17*, 126−135.
(23) Hayward, S., and Berendsen, H. J. (1998) Systematic analysis of domain motions in proteins from conformational change: new results on citrate synthase and T4 lysozyme. *Proteins 30*, 144−154.
(24) Tamura, K., Nei, M., and Kumar, S. (2004) Prospects for inferring very large phylogenies by using the neighbor-joining method. *Proc. Natl. Acad. Sci. U.S.A. 101*, 11030−11035.
(25) Mohammad-Qureshi, S. S., Jennings, M. D., and Pavitt, G. D. (2008) Clues to the mechanism of action of eIF2B, the guanine-nucleotide-exchange factor for translation initiation. *Biochem. Soc. Trans. 36*, 658−664.
(26) Hiyama, T. B., Ito, T., Imataka, H., and Yokoyama, S. (2009) Crystal structure of the alpha subunit of human translation initiation factor 2B. *J. Mol. Biol. 392*, 937−951.
(27) Pavitt, G. D., Ramaiah, K. V., Kimball, S. R., and Hinnebusch, A. G. (1998) eIF2 independently binds two distinct eIF2B subcomplexes that catalyze and regulate guanine-nucleotide exchange. *Genes Dev. 12*, 514−526.
(28) Holm, L., Kaariainen, S., Rosenstrom, P., and Schenkel, A. (2008) Searching protein structure databases with DaliLite v.3. *Bioinformatics 24*, 2780−2781.
(29) Gruber, J., Zawaira, A., Saunders, R., Barrett, C. P., and Noble, M. E. (2007) Computational analyses of the surface properties of protein-protein interfaces. *Acta Crystallogr. 63*, 50−57.
(30) Huberts, D. H., Venselaar, H., Vriend, G., Veenhuis, M., and van der Klei, I. J. (2010) The moonlighting function of pyruvate carboxylase resides in the non-catalytic end of the TIM barrel. *Biochim. Biophys. Acta 1803*, 1038−1042.
(31) Lucas, R., Magez, S., De Leys, R., Fransen, L., Scheerlinck, J. P., Rampelberg, M., Sablon, E., and De Baetselier, P. (1994) Mapping the lectin-like activity of tumor necrosis factor. *Science 263*, 814−817.
(32) Hundsberger, H., Verin, A., Wiesner, C., Pfluger, M., Dulebo, A., Schutt, W., Lasters, I., Mannel, D. N., Wendel, A., and Lucas, R. (2008) TNF: a moonlighting protein at the interface between cancer and infection. *Front. Biosci. 13*, 5374−5386.
(33) Yang, G., Hamacher, J., Gorshkov, B., White, R., Sridhar, S., Verin, A., Chakraborty, T., and Lucas, R. (2010) The dual role of TNF in pulmonary edema. *J. Cardiovasc. Dis. Res. 1*, 29−36.
(34) Christopher, S. A., Diegelman, P., Porter, C. W., and Kruger, W. D. (2002) Methylthioadenosine phosphorylase, a gene frequently codeleted with p16(cdkN2a/ARF), acts as a tumor suppressor in a breast cancer cell line. *Cancer Res. 62*, 6639−6644.
(35) Huberts, D. H., and van der Klei, I. J. (2010) Moonlighting proteins: an intriguing mode of multitasking. *Biochim. Biophys. Acta 1803*, 520−525.
(36) Kyte, J., and Doolittle, R. F. (1982) A simple method for displaying the hydropathic character of a protein. *J. Mol. Biol. 157*, 105−132.